Excitation functions for (p, n) reactions to 25 MeV on ^{63}Cu, ^{65}Cu, and ^{107}Ag†

R. Collé,* R. Kishore,‡ and J. B. Cumming
Chemistry Department, Brookhaven National Laboratory, Upton, New York 11973
(Received 3 December 1973)

Absolute cross sections for the (p,n) reactions on ^{63}Cu, ^{65}Cu, and ^{107}Ag at proton energies from 2.5 to 25 MeV were determined by the activation method. Metal foil targets of natural isotopic abundance were used; therefore, the results for ^{63}Zn above 22.3 MeV and for ^{107}Cd above 18.8 MeV include contributions from $(p, 3n)$ reactions. Beam intensities were measured with a Faraday cup. Disintegration rates of the product nuclei were determined by assaying their γ rays with calibrated Ge(Li) detector systems. Comparisons of the present cross sections are made with a complete compilation of previous measurements and with calculations based on a Monte Carlo intranuclear-cascade–statistical-evaporation model. Half-lives for ^{63}Zn and ^{107}Cd were determined to be 38.0 ± 0.1 min and 6.50 ± 0.02 h, respectively.

[NUCLEAR REACTIONS ^{63,65}Cu, ^{107}Ag(p, n), $E = 2.5$–25 MeV; measured $\sigma(E)$. Natural targets, Faraday cup, Ge(Li) detector. RADIOACTIVITY ^{63}Zn, ^{107}Cd; measured $T_{1/2}$.]

I. INTRODUCTION

Excitation functions for (p, n) reactions on Cu and Ag targets have been extensively studied both experimentally and theoretically for many years.[1–21] For some of these excitation functions there are well over 100 available cross-section measurements made by as many as 10 experimenters. The vast majority of these measurements however, are below 12 MeV. Furthermore, many of the previous measurements were beset with large uncertainties due to difficulties in the activity measurements and problems associated with the use of protons which had been degraded in energy by large factors. Nevertheless, because of this wealth of experimental data at low energies, these excitation functions have frequently been chosen for testing various theoretical models of nuclear reactions. In addition, Cu and Ag foils have commonly been used to monitor proton fluxes. As a result, many other excitation functions[22–24] are based on the absolute values of these cross sections. Unfortunately, the use of these excitation functions for comparisons with theoretical results or for beam monitoring has seldom relied on the full weight of all available data. In most cases, either only selected data or collections of previously reported values (uncorrected for systematic differences, such as in decay schemes, irrespective of changes over 20-yr periods of time) are used. Because of the importance of these excitation functions the present investigation was undertaken.

The excitation functions to 25 MeV for the ^{63}Cu$(p, n)^{63}$Zn, ^{65}Cu$(p, n)^{65}$Zn, and ^{107}Ag$(p, n)^{107}$Cd reactions were determined. The absolute activation cross-section measurements have uncertainties of approximately ±10% and energy uncertainties of ≈100 keV. This permits a critical evaluation of the previous work on these excitation functions.[1–4,8–14,18–20] For this a complete compilation, similar to one by Wing and Huizenga,[12] was made by renormalizing the reported values to remove systematic differences due to decay scheme changes. The higher-energy region (12–25 MeV), where previous data are rather scarce, is of special importance for comparisons to theoretical calculations. It is in this region of the excitation functions where several reactions [e.g., $(p, 2n)$, $(p, 3n)$, and (p, pn)] begin to compete strongly with the (p, n) reaction and where the (p, n) product can be formed by mechanisms other than compound nucleus. Early theoretical treatments in the low-energy region have mainly been concerned with predicting total reaction and compound-nucleus formation cross sections by optical-model calculations[9,11–13,19,20] or decay of the compound nucleus by simple statistical evaporation processes.[2,6,7,11,16] Of the more sophisticated calculations[25–34] which are applicable to the higher-energy region, very few comparisons have been made. A calculation based on the exciton model[33] has recently been made by Hille *et al.*[18] for the ^{63}Cu(p, n) excitation function. In the present study, the experimental excitation functions are compared to calculations based on a Monte Carlo intranuclear-cascade–statistical-evaporation model,[25–28] using the VEGAS code of Chen *et al.*[26] for the cascade stage and the DFF code of Dostrovsky, Fraenkel, and Friedlander[6] for the evaporation stage.

II. EXPERIMENTAL TECHNIQUES

The excitation functions were measured with proton beams from the Brookhaven tandem Van de Graaff accelerators in two-stage operation for energies up to 14 MeV and three-stage operation for energies from 14 to 25 MeV. The beam energy was controlled via voltage stabilizer feedback networks and analyzed to better than ±0.1% by a 90° analyzing magnet which was previously calibrated by proton magnetic resonance with the ^{12}C proton resonance at 14.231 ± 0.004 MeV.[35] In order to provide a large beam spot to minimize effects of possible small-scale nonuniformities of the targets, the beam was strongly defocused and diffused to greater than 1 cm diam. The beam was subsequently defined to 1 cm diam with a thick collimator which was insulated from the Faraday cup. The ratio of current on the collimator to that on target was typically 1:1. Crossed ≈1000-G magnetic fields provided by a set of permanent magnets located directly behind the collimator were used to suppress secondary electrons produced on the collimator edges. The Faraday cup with its magnet arrangement (shown in Fig. 1) was essentially based on the design criteria from a study by Cumming.[36] The aluminum cup is 14 cm deep × 7.5 cm diam and has a 2-cm-diam entrance aperture. An aluminum vacuum window at the end of the cup permitted free access to the target position without opening the cup to air for target changes. The size of the beam spot and the proper centering at the target position were established by monitoring the beam with a fluorescent quartz screen and closed-circuit TV camera. Then,

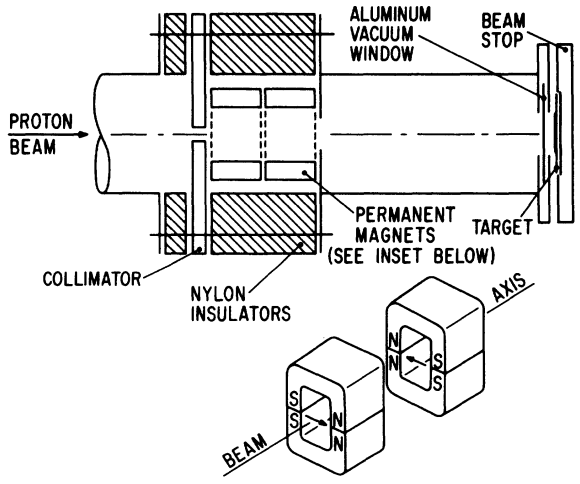

FIG. 1. Schematic of the Faraday cup. Details of the magnet arrangement used for secondary electron suppression are shown in the inset.

before each run, a trial irradiation was made with a piece of thin blue cellophane which discolors on irradiation. This provided an accurate representation of the beam location and area at the target position.

The total number of protons striking the target (i.e., total charge collected) during an irradiation was determined by integration of current from the Faraday cup. For each run, the current integrators were calibrated to an accuracy of better than ±0.3% with a standard current source. Furthermore, the following possible sources of systematic error were considered and excluded: (1) the current due to ionization of residual gas in the cup was necessarily small since a very good vacuum ($<10^{-5}$ Torr) was always maintained; (2) the effect of ionization in air outside the cup was demonstrated[36] to be negligible; (3) secondary electrons arising from the collimator were prevented from entering the cup; and (4) the escape of secondary electrons produced in the window or at the target position was rather improbable because of the geometrical arrangement and because the window was in electrical contact with the cup. As a result, the accuracy of the current integration is estimated to be ≈1%.

Energy degradation of the proton beam in the aluminum window (≈12.5 mg/cm^2), in the small air path (≈1.5 mg/cm^2), and in the targets was calculated from the range energy and stopping power (rate of energy loss dE/dx) tabulations of Northcliffe and Schilling[37] and Williamson, Boujot, and Picard.[38] To facilitate interpolation of their tables and to make consistent energy-loss corrections, logarithms of dE/dx as a function of energy were fitted to six-term polynomials. The fits were always better than (1.0–1.5%) for any of the absorbers in the energy range of interest (3–25 MeV). The mean energy of an irradiation was taken as the proton energy at the middle of the target. The error on the mean energy was obtained by quadratic propagation of the uncertainty in the incident beam energy, the error in the energy loss (due to both the uncertainty in thickness and in dE/dx) for each absorber and target, and the energy straggling[39] in each absorber and target. The uncertainties on the mean energies are typically 100 keV. Target thicknesses were in the range of 150 to 500 keV. However, even in the worst cases, corrections for this finite-energy resolution were negligible (<1%).

The targets of Cu and Ag were 5.2-cm^2 circular discs cut from high purity (>99.8%) 5- to 15-mg/cm^2 metallic foils with natural isotopic abundances. The thicknesses were determined to better than 1% by weighing. Although the beam averaged over a 0.79-cm^2 area of the target (see

above), the additional uncertainty due to possible small inhomogeneities and irregularities in the target surface was also considered in assigning an error of 1.0–1.5% in the number of target nuclei per unit area. Both single foils and stacks of three to six foils were used for the irradiations. Obviously, the irradiations of single foils are those with the best energy resolution, whereas the middle foils from stacked foil irradiations are those which require no correction for loss of reaction products by recoil. In all cases however, recoil losses were both estimated and empirically shown to be very small and were neglected in computing the cross sections.

Absolute disintegration rates of the product nuclei were assayed without chemical separation, since the different half-lives and distinct γ-ray energies were sufficient to distinguish and identify them by high-resolution γ-ray spectroscopy. The principal radioactive decay characteristics of the product nuclei which were used in this work are given in Table I. For ^{63}Zn, the averages from assaying both the 669.6- and 961.9-keV γ rays were used for the determinations. Measurements were made with Ge(Li) coaxial detectors and 4096-channel pulse-height analyzers which were previously calibrated[44] for efficiency (at fixed counting geometries) with absolute International Atomic Energy Agency and National Bureau of Standards standard sources. Multiple spectra of each source at a fixed counting geometry were taken as a function of time. To minimize systematic errors, analyzer dead times were usually kept less than 5%. Copper absorbers (369 mg/cm^2) were placed over the sources in order to annihilate the β^+ radiation at the sources and prevent the positrons from entering the detector, and to attenuate the x rays to minimize coincident summing with γ rays. Analysis of the γ-ray spectra was performed by means of a modified version of the BRUTAL[45] computer code. The resultant decay curves were analyzed by a least-squares procedure using the CLSQ[46] program. The maximum statistical uncertainty on any of the data points (i.e., γ-ray peak intensities) used in the decay curve analyses was 3%. The data were fitted to the known half-lives (see Table I) to obtain the extrapolated counting rates at the end of irradiation. These were converted to absolute disintegration rates by applying the efficiencies and γ-ray abundances (see Table I), and correcting for absorption in both the source and the Cu absorber, and for summation of coincident γ-ray, x-ray, and annihilation radiation.

TABLE I. Radioactive decay characteristics of the product nuclei which were used for the cross-section measurements in this work.

Product nucleus	Half-life	γ-ray energy (keV)	γ-ray abundance (photons/100 disintegrations)
^{63}Zn	38.0 ± 0.1 min [a]	669.6	8.47 ± 0.33 [b]
		961.9	6.68 ± 0.19 [b]
^{65}Zn	243.8 ± 0.7 day [c]	1115.4	50.6 ± 0.4 [c]
^{107}Cd	6.50 ± 0.02 h [a]	93.1	4.76 ± 0.07 [d]

[a] See Appendix.
[b] Reference 41.
[c] Reference 40.
[d] Obtained from combining the total transition intensity (0.99937 transitions per disintegration) given in Ref. 42 with the total theoretical internal-conversion coefficient (α = 20.0) for an $E3$ multipole transition given in Ref. 43.

Absolute cross sections were calculated from these disintegration rates, the number of target nuclei per unit area, and the number of incident protons. The irradiations were of sufficiently short duration compared to the half-lives of interest so that variations in beam intensity had a negligible effect (<2%) on the derived cross sections. The uncertainties in the cross sections include the errors in the peak analyses including counting statistics (always <3%), decay curve analyses (typically <3%), absolute detector efficiencies (5–10%), γ-ray abundances (1–4%), target thicknesses (≈1.0–1.5%), and current integration (≈1%). The over-all uncertainties were obtained by combining the above errors in quadrature and are typically of the order ±(7–12%). The cross sections relative to each other would have considerably smaller errors however, since the systematic uncertainties in the detector efficiencies and γ-ray abundances would be removed.

III. RESULTS AND DISCUSSION

A. Experimental cross sections

The experimental cross sections for the ^{63}Cu$(p, n)^{63}$Zn and ^{65}Cu$(p, n)^{65}$Zn, and ^{107}Ag$(p, n)^{107}$Cd reactions are tabulated in Tables II and III, respectively. For ^{63}Zn and ^{107}Cd, the cross sections at high energies also include the contributions from $(p, 3n)$ reactions on ^{65}Cu and ^{109}Ag, respectively. These cross sections along with all of the values from previous measurements have been plotted as excitation functions in Figs. 2–4. Because of the wealth of previous data, especially at low energies (<12 MeV), the data points are not individually identified in the figures. Brief summaries of the previous measurements[1–4,8–14,18–20] whose results are included in Figs. 2–4 are tabulated in Table IV. For each study, the table contains the experimental method used for the measurements (including relevant decay scheme data and calibration information), the method of beam monitoring, the incident proton energy and energy

range of the measurements, and the number of cross sections which were determined. The compilation includes measurements by both activation and neutron detection methods. Measurements by neutron detection in which targets with natural isotopic abundances were employed[7,15,16] were not included. The activation measurements were renormalized when necessary to base them on the same decay schemes. The conversion factors used to make these corrections are also given in Table IV (column 5). For those activation measurements where the available information was insufficient to make the correction and for the neutron detection measurements, the conversion factor is unity.

As indicated in Figs. 2–4, the present results are in good agreement with the vast majority of the previous work. The only notable exception is the high-energy region (>14 MeV) of the ^{63}Cu(p,n)-^{63}Zn reaction excitation function (Fig. 2) where the cross sections obtained by Ghoshal[1] and Meadows[3] are considerably larger than the present results. Both of these studies utilized proton beams which had been degraded in energy by large factors (see Table IV) and thus are subject to substantial energy uncertainties. Hille *et al.*[18] have suggested that the Ghoshal data[1] should be shifted to lower energy by 1 to 1.5 MeV because of possible errors in the energy-loss calculations which may have resulted from the use of old stopping-power values. A shift of 1 MeV would put the majority of Ghoshal's data in reasonable agreement with the present results. The cross sections obtained by Meadows[3] are systematically higher than the present data and all of the other previous work. This has

TABLE II. Experimental cross sections for production of ^{63}Zn and ^{65}Zn.

E_p (MeV)	$\sigma(^{63}\mathrm{Zn})$ (mb)	$\sigma(^{65}\mathrm{Zn})$ (mb)	E_p (MeV)	$\sigma(^{63}\mathrm{Zn})$ (mb)	$\sigma(^{65}\mathrm{Zn})$ (mb)
2.86	...	14.0± 0.7	15.45	264 ±19	243 ±11
3.70	...	73.0± 3.4	15.87	243 ±17	211 ±11
3.89	...	91.4± 4.4	16.04	227 ±17	204 ±11
3.99	0.013± 0.002	95.1± 4.7	16.20	218 ±16	201 ±10
4.32	10.2 ± 0.8	130 ± 7	16.64	186 ±14	165 ± 8
4.63	49.6 ± 3.8	171 ± 8	16.81	173 ±13	165 ±10
4.99	89.4 ± 6.6	221 ±10	16.97	166 ±12	156 ± 8
5.11	115 ± 8	250 ±14	18.48	100 ± 7	93.1± 4.5
6.16	205 ±15	422 ±24	18.70	87.4± 6.6	88.7± 5.1
7.23	262 ±20	492 ±30	18.85	90.7± 6.8	89.5± 4.4
8.29	334 ±25	559 ±32	19.01	85.6± 6.4	86.5± 4.4
9.20	367 ±27	697 ±32	19.73	71.1± 5.3	72.6± 3.5
9.37	404 ±27	644 ±35	19.86	65.8± 4.9	69.4± 4.0
10.33	421 ±31	731 ±40	20.00	63.7± 4.8	68.8± 3.4
11.29	426 ±31	731 ±34	21.51	45.1± 3.3	53.6± 2.8
11.36	466 ±32	716 ±40	22.37	40.4± 3.1[a]	45.9± 2.8
12.52	437 ±32	576 ±33	22.49	41.9± 3.2[a]	42.0± 3.1
12.63	465 ±34	560 ±46	22.62	39.3± 3.1[a]	46.1± 1.0
12.83	458 ±33	550 ±26	23.24	35.6± 2.8[a]	41.0± 1.0
13.02	459 ±33	456 ±26	23.37	33.7± 2.5[a]	40.8± 2.3
13.07	500 ±34	493 ±27	23.51	34.4± 2.7[a]	42.7± 2.7
13.17	488 ±38	530 ±32	25.02	33.3± 2.5[a]	34.1± 1.9
13.21	467 ±35	527 ±30			
13.37	455 ±34	500 ±25			
13.50	424 ±32	439 ±24			
13.52	423 ±30	440 ±24			
13.56	457 ±34	481 ±29			
14.07	413 ±31	390 ±19			
14.25	394 ±29	340 ±18			
14.44	386 ±28	357 ±18			

[a] ^{65}Cu(p,$3n$)^{63}Zn reaction contributes (reaction threshold = 22.31 MeV); apparent cross section is

$$\sigma(^{63}\mathrm{Zn}) = \sigma[^{63}\mathrm{Cu}(p,n)] + \frac{N(^{65}\mathrm{Cu})}{N(^{63}\mathrm{Cu})}\,\sigma[^{65}\mathrm{Cu}(p,3n)].$$

also been observed by Newton *et al.*[49] for several other excitation functions reported in Meadows's study.[3] The recent measurements by Hille *et al.*[18] for the $^{63}Cu(p, n)^{63}Zn$ reaction cross sections are also systematically too high although by much smaller percentages (10–25%). Since the experimental techniques of their study and the present work were nearly identical these discrepancies are rather unexpected. Both the $^{63}Cu(p, n)^{63}Zn$ and $^{65}Cu(p, n)^{65}Zn$ reaction cross sections at 9.85 MeV measured by Jones and Schiffer[10] appear to be too low by approximately 20–25%. The ratio of these cross sections however, is in good agreement with the present work and that of Refs. 4, 9, 11, and 12, therefore suggesting the possibility of a systematic calibration error in their experiment. Beside that of Jones and Schiffer,[10] the only other cross sections in the $^{65}Cu(p, n)^{65}Zn$ reaction excitation function (Fig. 3) which are not in good agreement with the bulk of the other data are the very low-energy (<4-MeV) measurements of

TABLE III. Experimental cross sections for production of ^{107}Cd.

E_p (MeV)	σ (mb)	E_p (MeV)	σ (mb)
2.51	0.019± 0.002	13.46	390 ±26
3.12	0.52 ± 0.04	13.58	370 ±25
3.65	1.82 ± 0.13	13.99	314 ±21
3.84	2.52 ± 0.17	14.39	267 ±18
4.16	5.16 ± 0.35	15.59	154 ±11
4.94	24.4 ± 1.6	15.95	144 ±10
6.06	101 ± 7	16.19	132 ± 9
7.20	216 ±15	16.45	110 ± 7
8.17	331 ±20	16.69	104 ± 7
9.18	521 ±36	16.92	96.4± 6.5
9.35	495 ±47	18.71	54.8± 3.8
10.30	606 ±41	19.04	51.1± 3.7 [a]
10.31	644 ±55	19.27	48.5± 3.3 [a]
11.33	664 ±46	19.50	46.0± 3.2 [a]
11.34	680 ±47	19.73	47.3± 3.2 [a]
12.29	548 ±37	19.96	50.9± 3.5 [a]
12.43	496 ±33	22.43	263 ±18 [a]
12.58	491 ±34	22.73	293 ±20 [a]
12.62	518 ±35	22.92	346 ±25 [a]
12.95	460 ±31	23.12	357 ±24 [a]
12.99	449 ±31	23.40	392 ±27 [a]
13.27	386 ±26		
13.27	402 ±28		
13.44	369 ±36		
13.44	373 ±25		

[a] $^{109}Ag(p, 3n)^{107}Cd$ reaction contributes (reaction threshold = 18.83 MeV); apparent cross section is

$$\sigma(^{107}Cd) = \sigma[^{107}Ag(p,n)] + \frac{N(^{109}Ag)}{N(^{107}Ag)}\sigma[^{109}Ag(p, 3n)].$$

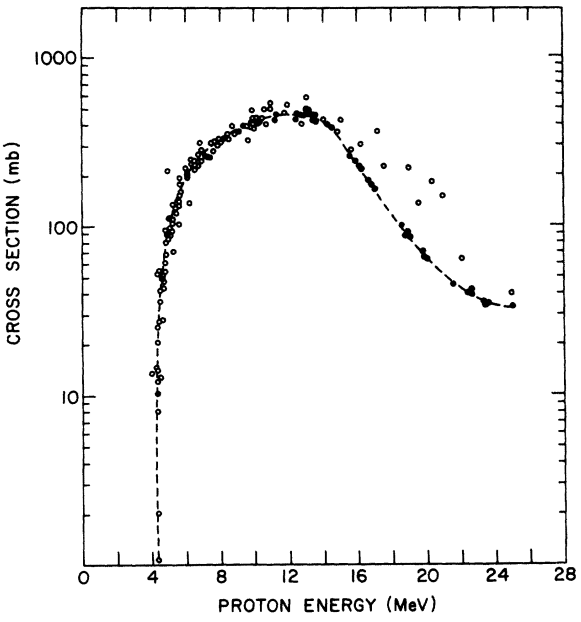

FIG. 2. Experimental excitation function for the $^{65}Cu(p,n)^{63}Zn$ reaction. The closed circles represent the results from the present measurements. The open circles are renormalized values of previous measurements (see Table IV and text). Cross sections from the present work above 22 MeV include the contribution from the $^{65}Cu(p, 3n)^{63}Zn$ reaction.

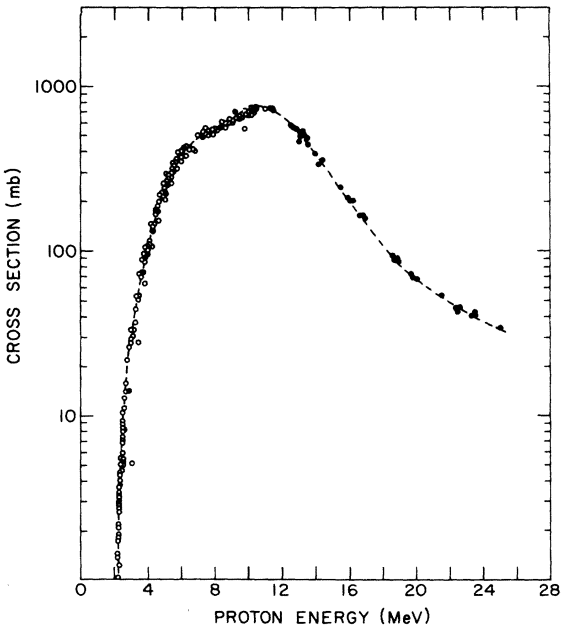

FIG. 3. Experimental excitation function for the $^{65}Cu(p,n)^{65}Zn$ reaction. The closed circles represent the results from the present measurements. The open circles are renormalized values of previous measurements (see Table IV and text).

TABLE IV. Summary of previous measurements of (p,n) reaction cross sections on ^{63}Cu, ^{65}Cu, and ^{107}Ag.

Author identification	Ref.	Method [a] (detector, radiation detected, % decay, calibration, etc.)	Conversion factor [b]	Beam monitoring	Incident proton energy and energy range of measurements	No. of cross sections determined
			^{63}Cu target			
Ghoshal (1950)	1	A; Geiger counter; β^+; $I_{\beta^+}=85\%$	0.916 [c]	Faraday cup	32 MeV degraded, 3.9 to 22.1 MeV	18
Blaser (1951)	2	A; Geiger counter; β^+; $I_{\beta^+}=85\%$; calibrated with NBS Ra($D+E$) Std.	0.916 [c]	Faraday cup	6.5 MeV degraded, 4.2 to 6.3 MeV	9
Meadows (1953)	3	A; Geiger counter; β^+	1.0 [d]	$^{27}Al(p,3pn)^{24}Na$ cross sections calibrated by $^{12}C(p,pn)^{11}C$ cross sections [f]	100 MeV degraded, 5.0 to 25.0 MeV [e]	8 [e]
Howe (1958)	4	A; NaI(Tl) coincidence counting of β^+ annihilation radiation; $I_{\beta^+}=89.3\%$; calibrated with NBS ^{22}Na std.	0.962 [c]	Faraday cup	20 MeV degraded, 4.5 to 10.3 MeV	14
Johnson (1960)	8	N; 4π graphite-sphere detector	1.0	Faraday cup	Variable; 4.24 to 5.78 MeV	29
Albert (1961)	9	N; $^{10}BF_3$ counter [g]	1.0	Faraday cup	9.85 MeV	1
Jones (1961)	10	N; $^{10}BF_3$ counter	1.0	...	9.85 MeV	1
Hansen (1962)	11	N; $^{10}BF_3$ counter; calibrated with with NBS Po-Be std.	1.0	Faraday cup	Variable, 6.0 to 11.0 MeV	6
Wing (1962)	12	A; NaI(Tl) coincidence counting of β^+ annihilation radiation; $I_{\beta^+}=93\%$; calibrated with ^{22}Na std.	1.002 [c]	Faraday cup	10.5 MeV degraded, 4.5 to 10.5 MeV	22
Taketani (1962)	13	A; NaI(Tl) coincidence counting of β^+ annihilation radiation; $I_{\beta^+}=89.8\%$, calibrated with NBS ^{22}Na std.	0.968 [c]	Faraday cup calibrated with std. current source	Variable, 4.2 to 6.6 MeV	6
Taketani (1962)	13	N; $^{10}BF_3$ counter	0.968	$^{63}Cu(p,n)^{63}Zn$ cross sections calibrated by foil activation	Variable, 4.4 to 6.6 MeV	4
Humes (1963)	14	N; NaI(Tl) detector; γ rays; calculated efficiencies	1.0 [d]	Faraday cup	6.75 MeV	1
Hille (1972)	18	N; Ge(Li) detector; 669.6-keV γ ray; $I_\gamma=10.1\%$; calibrated with IAEA stds.	1.192 [h]	Faraday cup	16 MeV degraded, 8.7 to 15.8 MeV	8
			^{65}Cu target			
Blaser (1951)	2	N; Geiger counter; β^+ and γ rays; assumed 46% E.C. to 1.12-MeV state, 54% E.C. to ground state, 2.2% β^+	0.889 [i]	Faraday cup	6.5 MeV degraded, 2.8 to 6.3 MeV	11
Howe (1958)	4	A; NaI(Tl) coincidence counting of β^+ annihilation radiation; relative cross sections normalized to Blaser (1951) value at 6.3 MeV	0.889	Faraday cup	20 MeV degraded, 6.4 to 11.4 MeV	5

TABLE IV *(Continued)*

Author identification	Ref.	Method [a] (detector, radiation detected, % decay, calibration, etc.)	Conversion factor [b]	Beam monitoring	Incident proton energy and energy range of measurements	No. of cross sections determined
Johnson (1958)	19	N; 4π detector of $^{10}BF_3$ counters embedded in paraffin; calibrated with Mn bath against NBS Ra-Be std.	1.0	Faraday cup	Variable, 2.17 to 2.54 MeV	45
Johnson (1960)	8	N; 4π graphite-sphere detector [j]	1.0	Faraday cup	Variable, 2.23 to 5.78 MeV	64
Jones (1961)	10	N; $^{10}BF_3$ counter	1.0	...	9.85 MeV	1
Shore (1961)	20	A; NaI(Tl) coincidence counting of x-ray–1115-keV γ ray; calibrated with NBS ^{65}Zn std.	0.968 [i]	Faraday cup	7.5 MeV	1
Albert (1961)	9	N; $^{10}BF_3$ counter	1.0	Faraday cup	9.85 MeV	1
Hansen (1962)	11	N; $^{10}BF_3$ counter; calibrated with NBS Po-Be std.	1.0	Faraday cup	Variable, 6.0 to 11.0 MeV	6
Wing (1962)	12	A; NaI(Tl) detector; 1115-keV γ ray; $I_\gamma = 49\%$; calibrated with ^{46}Sc source assuming one 1.12-MeV γ ray per disintegration	0.968 [i]	Faraday cup	10.5 MeV degraded, 4.5 to 10.5 MeV	42
Humes (1963)	14	A; NaI(Tl) detector; γ rays; calculated efficiencies	1.0 [d]	Faraday cup	6.75 MeV	1
			^{107}Ag target			
Blaser (1951)	2	A; Geiger counter; K x rays from internal conversion of 93-keV transition; $\alpha = 16 \pm 3$	1.235 [k]	Faraday cup	6.5 MeV degraded, 3.3 to 6.4 MeV	18
Johnson (1960)	8	N; 4π graphite-sphere detector	1.0	Faraday cup	Variable, 2.08 to 5.82 MeV	16
Wing (1962)	12	A; NaI(Tl) detector; 93-keV γ ray; $I_\gamma = 4.9\%$; calculated efficiencies	1.035 [k]	Faraday cup	10.5 MeV degraded, 1.9 to 10.5 MeV	24

[a] A refers to measurements by activation method and N by neutron detection.

[b] A normalization factor used to put the previous results on the same basis of decay scheme. For example, Ghoshal's data for the $^{63}Cu(p,n)$ reaction must be corrected by the ratio 85/92.8 since he assumed 85% β^+ emission in ^{63}Zn while the present value is 92.8%.

[c] Present value $I_{\beta^+} = 92.8\%$ taken from Ref. 41.

[d] Available information is insufficient to make conversion.

[e] Eight additional cross sections from 31.2 to 99.2 MeV were also determined.

[f] Monitor cross sections taken from Ref. 47.

[g] Their cross section has been revised from 510 to 450 mb, see note in Ref. 12.

[h] Present value $I_\gamma = (8.47 \pm 0.33)\%$, see Table I.

[i] Present decay scheme: 50.6% E.C. to 1.12-MeV state, 48% E.C. and 1.54% β^+ to ground state, see Table I and Ref. 40.

[j] Their cross sections have been increased by a factor of 1.43, see note in Ref. 48.

[k] Present values $\alpha = 20.0$ and $I_\gamma = (4.76 \pm 0.04)\%$, see Table I.

Blaser *et al.*[2] Their low-energy data points are slightly displaced to the higher-energy side and it undoubtedly results from the energy uncertainty in degrading the fixed energy proton beam to low energies. Above 12 MeV, no previous measurements on either the $^{65}Cu(p, n)^{65}Zn$ or $^{107}Ag(p, n)^{107}Cd$ reaction excitation functions are available. The present results have extended these excitation functions into this theoretically interesting higher-energy region. For the $^{107}Ag(p, n)^{107}Cd + ^{109}Ag(p, 3n)^{107}Cd$ excitation function (Fig. 4), the increase above 20 MeV is due to the rapidly increasing $(p, 3n)$ reaction cross sections. The threshold for this reaction is ≈18.3 MeV.

B. Calculated cross sections

The calculated excitation functions based on a Monte Carlo intranuclear-cascade–statistical-evaporation model[6,25-28] are compared to the experimental curves in Figs. 5–7. The cascade stage was calculated with one of the STEP versions of the VEGAS code.[26] In this version, the nuclear density distribution consisted of seven concentric spherical shells of constant density and potential which approximate the Fermi density distribution. Refinements in the model for refraction and reflection of cascade nucleons at the boundaries of each constant potential region (step)[26] and for velocity-dependent potentials[27] were not included since these more sophisticated and complex versions have earlier been shown to have only limited success.[23,28] Typically, 1000 cascades were performed for each incident proton energy at intervals of 2–3 MeV starting from ≈13 MeV. Ten evaporation sequences were calculated for each of the excited residual nuclei with the DFF code, which is based on the Monte Carlo formalism of Dostrovsky, Fraenkel, and Friedlander (DFF).[6] For the calculations, the level density parameter was set equal to $A/20$, the binding energies and masses were taken from the 1962 compilation of Konig, Mattauch, and Wapstra,[50] a reduced radius of $r_0 = 1.5$ fm was used for calculating the inverse reaction cross sections for particle emission, and

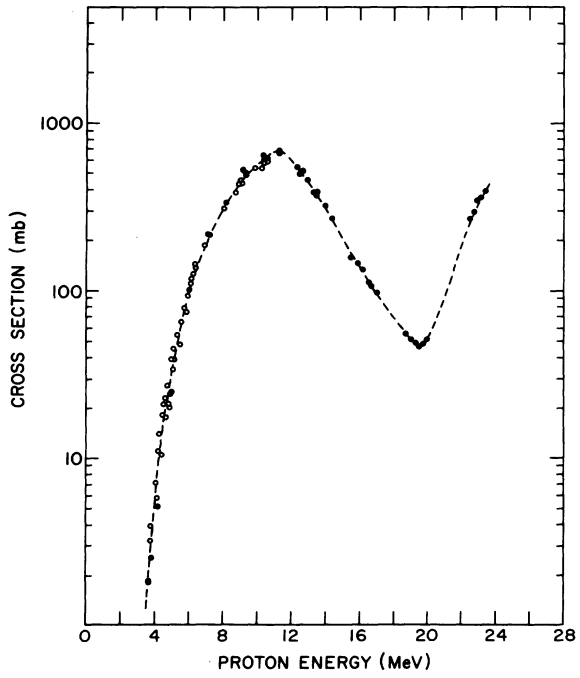

FIG 4. Experimental excitation function for the $^{107}Ag(p, n)^{107}Cd + ^{109}Ag(p, 3n)^{107}Cd$ reactions. The closed circles represent the results from the present measurements. The open cirlces are renormalized values of previous measurements (see Table IV and text). Above ≈ 18.8 MeV, the cross section for production of ^{107}Cd is the weighted sum of the (p, n) and $(p, 3n)$ reaction cross sections. The sharp rise in the excitation function results from the rapidly increasing $(p, 3n)$ cross section.

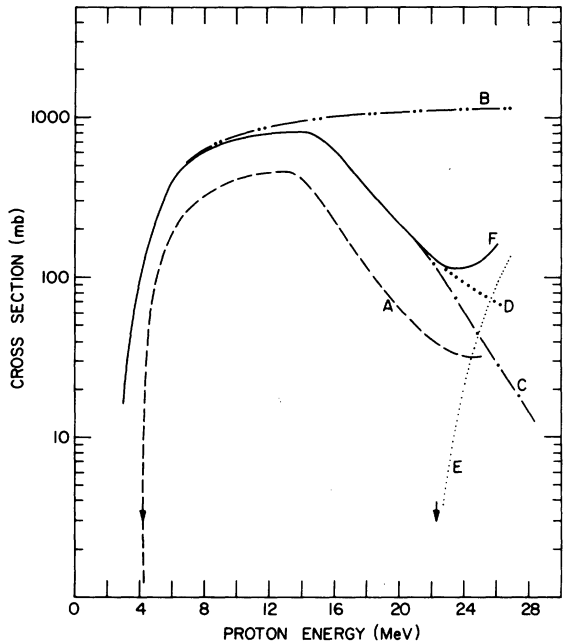

FIG. 5. Comparison of experimental $^{63}Cu(p, n)^{63}Zn$ reaction excitation function with evaporation and cascade-evaporation calculations. The labeled curves are: A, experimental excitation function given in Fig. 2; B, ^{63}Cu optical-model reaction cross sections taken from Ref. 51; C, DFF evaporation calculations for $^{63}Cu(p, n)$; D, VEGAS-DFF cascase-evaporation calculations for $^{63}Cu(p, n)$; E, VEGAS-DFF cascade-evaporation calculations for $^{65}Cu(p, 3n)$; F, weighted sum of curves D and E. The $^{63}Cu(p, n)$ and $^{65}Cu(p, 3n)$ reaction thresholds at 4.21 and 22.3 MeV, respectively, are labeled with arrowheads.

the pairing energies were those given in their work.[6] The DFF code was also used for pure compound-nucleus–statistical-evaporation calculations at 1-MeV intervals over the entire energy range of the excitation functions. From 1000 to 7000 evaporations were performed at each incident energy. For either the cascade evaporation or simple evaporation case, DFF calculation provided the fractional probabilities for production of a given product nucleus per incident proton. The maximum statistical uncertainties on these probabilities for the cascade-evaporation calculations were of the order 5–15%, and for the evaporation calculations were usually much less than 10%, except at very high energies where it gradually increased to 30% since very few events proceeded to the (p, n) reaction products. The probabilities were converted to production cross sections using the optical-model reaction cross sections given by Mani, Melkanoff, and Iori.[51] It should be emphasized that at no stage of the calculation are the calculated cross sections arbitrarily normalized to experimental data.

In Figs. 5–7, the curves labeled A, B, C, and D are, respectively, the experimental excitation functions taken from Figs. 2–4, the optical-model reaction cross sections,[51] the DFF evaporation calculations, and the VEGAS-DFF cascade-evaporation calculations. Figures 5 and 7 also contain VEGAS-DFF calculations (labeled curves E) for the ^{65}Cu$(p, 3n)^{63}$Zn and ^{109}Ag$(p, 3n)^{107}$Cd reaction excitation functions. The thresholds, labeled in the figures with arrowheads, for these $(p, 3n)$ reactions are 22.3 and 18.8 MeV, respectively. The weighted sums of the (p, n) and $(p, 3n)$ reaction cross sections are given in the figures as the curves labeled F.

The results from both the simple evaporation and cascade-evaporation calculations are virtually identical up to energies several (2–4) MeV beyond the peaks of the excitation functions. This agreement is simply a natural result of the fact that up to these energies the cascade calculation predicts the formation of a compound nucleus for nearly every inelastic event. Above this, the evaporation

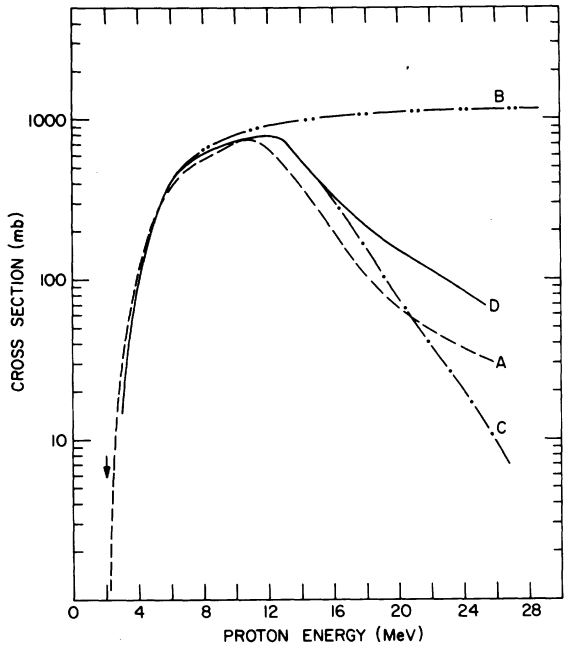

FIG. 6. Comparison of experimental ^{65}Cu$(p, n)^{65}$Zn reaction excitation function with evaporation and cascade-evaporation calculations. The labeled curves are: A, experimental excitation function given in Fig. 3; B, ^{65}Cu optical-model reaction cross sections taken from Ref. 51; C, DFF evaporation calculations for ^{65}Cu(p, n); D, VEGAS-DFF cascade-evaporation calculations for ^{65}Cu(p, n). The reaction threshold at 2.17 MeV is labeled with an arrowhead.

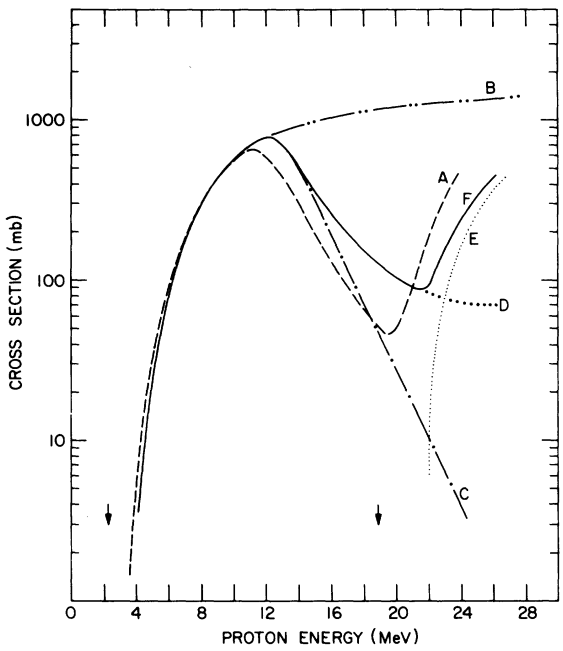

FIG. 7. Comparison of experimental ^{107}Ag$(p, n)^{107}$Cd $+^{109}$Ag$(p, 3n)^{107}$Cd reaction excitation function with evaporation and cascade-evaporation calculations. The labeled curves are: A, experimental excitation function given in Fig. 4; B, ^{107}Ag optical-model reaction cross sections taken from Ref. 51; C, DFF evaporation calculations for ^{107}Ag(p, n); D, VEGAS-DFF cascade-evaporation calculations for ^{107}Ag(p, n); E, VEGAS-DFF cascade-evaporation calculations for ^{109}Ag$(p, 3n)$; F, weighted sum of curves D and E. The ^{107}Ag(p, n) and ^{109}Ag$(p, 3n)$ reaction thresholds at 2.22 and 18.8 MeV, respectively, are labeled with arrowheads.

calculation predicts a steady decrease in the cross section with increasing energy, while the cascade-evaporation calculation predicts a slower, more gradual tailing in the excitation function due to direct processes which also lead to the (p, n) product. These qualitative features are similar to those of several previous reports.[22,23]

The peak cross sections for the $^{65}Cu(p, n)^{65}Zn$ (Fig. 6) and $^{107}Ag(p, n)^{107}Cd$ reactions (Fig. 7) excitation functions agree reasonably well with the calculations, whereas, for the $^{63}Cu(p, n)^{63}Zn$ excitation function (Fig. 5), the calculated cross sections are nearly a factor of 2 larger than the experimental values. Neglecting the magnitude of the cross sections, the general shape of the excitation functions appear to be reproduced by the cascade-evaporation calculations. For even the two former cases (Figs. 6 and 7) however, the calculations systematically overestimate the cross sections on the high-energy side of the peaks. Furthermore, the predicted peak positions are consistently about 1 MeV too high. Although not readily apparent in Figs. 5 and 6, this shift in peak position can easily be seen in Fig. 7. This 1-MeV shift in the $^{107}Ag(p, n)$ reaction peak position manifests itself as a ≈2-MeV shift in the valley at ≈20 MeV [due to the decreasing $^{107}Ag(p, n)$ and increasing $^{109}Ag(p, 3n)$ reaction cross sections]. Some of the small systematic disagreements between the calculated and experimental excitation functions are ascribable to the parameters which enter into the calculation. For example, the peak position and shape of the excitation function are dependent on the value of the level density parameter a. An increase in a, such as from $A/20$ to $A/10$, would have the effect of shifting the evaporated particle spectrum to lower energies because of the decrease in nuclear temperature. As a consequence, the rising and falling edges of the peak would become sharper and the peak position would be shifted to lower energy. These effects of a on the results from evaporation calculations have been demonstrated by Dostrovsky, Fraenkel, and Friedlander.[6] Similarly, the magnitude of the cross sections at the peak positions can be changed by varying the values of the pairing energy terms δ or the value of the reduced radius r_0. Although minor variations of these parameters may have some slight beneficial effect on the results of the calculation, it would not substantially change the over-all trends. The present overestimation of the cross sections at the higher energies can be contrasted to the underestimation (to about the same degree) observed in previous similar calculations on other (p, n) reaction excitation functions.[22,23] These previous studies used a version of the VEGAS cascade calculation which included reflection and refraction of the cascade nucleons. These trends suggest that the fraction of compound-nucleus formation at higher energies is overestimated in the latter versions, while in the former versions (present work) it is underestimated.

ACKNOWLEDGMENTS

The authors would like to thank S. Katcoff for valuable discussions throughout the course of this work and for his thoughtful criticism of the manuscript during its preparation. Special thanks are due George Harp for help in carrying out the VEGAS and DFF calculations and for discussions of the calculations. Assistance provided by D. E. Alburger and the staff of the Brookhaven tandem Van de Graaff accelerators in obtaining irradiations is gratefully acknowledged.

TABLE V. Half-lives of ^{63}Zn and ^{107}Cd.

	E_γ (keV)	No. decay curves	Weighted mean $T_{1/2}$ [a]	$\hat{\sigma}$ [b]	$T_{1/2}$ [c]
^{63}Zn	669.6	17	38.06 ± 0.09 min	2.33	38.1 ± 0.2 min
	961.9	17	37.96 ± 0.11 min	1.56	38.0 ± 0.2 min
	all	34	38.02 ± 0.07 min	1.96	38.0 ± 0.1 min
^{107}Cd	93.1	14	6.504 ± 0.004 h	5.16	6.50 ± 0.02 h
	324.6	5	6.546 ± 0.041 h	1.96	6.55 ± 0.08 h
	422.6	3	6.552 ± 0.048 h	1.14	6.55 ± 0.06 h
	796.4	4	6.389 ± 0.045 h	2.22	6.39 ± 0.10 h
	828.9	4	6.466 ± 0.033 h	1.47	6.47 ± 0.05 h
	all	30	6.503 ± 0.004 h	3.69	6.50 ± 0.02 h

[a] Weighted (inverse square of standard deviations) mean of the fitted half-lives.

[b] Goodness-of-fit parameter for the weighted mean as given in Ref. 52.

[c] Assigned half-life; the reported error was obtained from the product of the goodness-of-fit parameter for the mean and the statistical uncertainty on the mean, see text.

APPENDIX

As an outgrowth of the present investigation, the half-lives for ^{63}Zn and ^{107}Cd were determined from the numerous γ-ray decay curves which were obtained in the course of this work. The target irradiations, γ-ray spectrometry, and decay curve analyses were described in Sec. II.

For ^{63}Zn, decay curves for the 669.6- and 961.9-keV γ rays were followed for two to eight half-lives. In all, 34 decay curves with a combined total of 335 data points were analyzed. The unweighted mean of these 34 least-squares-fitted half-lives is 38.1 ± 0.2 min. Weighted (inverse square of the standard deviations) means with their one standard deviation (σ) statistical uncertainties were also obtained and are provided in Table V. The reported errors on $T_{1/2}$ were obtained from the product of the goodness-of-fit parameter[52] ($\hat{\sigma}$) for the weighted means and the statistical uncertainty (σ) on the means. The result obtained for the half-life of ^{63}Zn is

$$T_{1/2}(^{63}\mathrm{Zn}) = 38.0 \pm 0.1 \text{ min}.$$

Agreement is generally good with previously reported values: 38.3 min,[53-55] 38.3 ± 0.5 min,[56] 38.0 ± 1.3 min,[57] 38.5 ± 0.8 min,[58] 38.1 ± 0.3 min,[59] 36 ± 2 min,[60] 39.9 ± 0.8 min,[61] 37.6 ± 0.3 min,[62] 38.4 ± 0.2 min,[63] 39.0 ± 0.1 min,[64] 38.40 ± 0.05 min,[65] and 38.5 ± 0.1 min.[41]

For the ^{107}Cd half-life determination the intense 93.1-keV γ ray was primarily used. For several of the sources however, additional decay curves were also obtained for the weaker 324.6-, 422.6-, 796.4-, and 828.9-keV γ rays. 30 decay curves followed for two to six half-lives with a combined total of 540 data points were obtained. The unweighted mean half-life from these 30 measurements is 6.47 ± 0.05 h. The various weighted mean half-lives are also given, as for ^{63}Zn, in Table V. These results indicate that the half-life of ^{107}Cd is

$$T_{1/2}(^{107}\mathrm{Cd}) = 6.50 \pm 0.02 \text{ h}.$$

Previously reported values for this half-life include: 6.7 h,[58,66] 6.4 h,[67] and 6.49 ± 0.05 h.[68]

Values for the ^{63}Zn and ^{107}Cd half-lives adopted in recent compilations[42,69] are 38.4 min and 6.5 h, respectively. Our result for ^{63}Zn suggests that the half-life is shorter than the adopted value. In the case of ^{107}Cd, our result is in excellent agreement with the other existing precision measurement[68] which suggests that the adopted value should be revised to reflect this higher precision.

---

†Research supported by Advanced Research Projects Agency (ARPA Order No. 1590) and the U.S. Atomic Energy Commission.

*Present address: Department of Chemistry, University of Maryland, College Park, Maryland 20742.

‡Present address: Department of Radiopharmacy, Harvard Medical School, Boston, Massachusetts 02115.

[1]S. N. Ghoshal, Phys. Rev. 80, 939 (1950).

[2]J. P. Blaser, F. Boehn, P. Marmier, and D. C. Peaslee, Helv. Phys. Acta 24, 3 (1951).

[3]J. W. Meadows, Phys. Rev. 91, 885 (1953).

[4]H. A. Howe, Phys. Rev. 109, 2083 (1958).

[5]G. A. Jones, Nucl. Phys. 12, 167 (1958).

[6]I. Dostrovsky, Z. Fraenkel, and G. Friedlander, Phys. Rev. 116, 683 (1959).

[7]R. L. Bramblett and T. W. Bonner, Nucl. Phys. 20, 395 (1960).

[8]C. H. Johnson, A. Galonsky, and C. N. Inskeep, Oak Ridge National Laboratory Report No. ORNL-2910, 1960 (unpublished), p. 25.

[9]R. D. Albert and L. F. Hansen, Phys. Rev. Lett. 6, 13 (1961); Phys. Rev. 123, 1749 (1961).

[10]G. A. Jones and J. P. Schiffer, Bull. Am. Phys. Soc. 6, 273 (1961).

[11]L. F. Hansen and R. D. Albert, Phys. Rev. 128, 291 (1962).

[12]J. Wing and J. R. Huizenga, Phys. Rev. 128, 280 (1962).

[13]H. Taketani and W. P. Alford, Phys. Rev. 125, 291 (1962).

[14]R. M. Humes, G. F. Dell, Jr., W. D. Ploughe, and H. J. Hausman, Phys. Rev. 130, 1522 (1963).

[15]R. G. Thomas, Jr., and W. Bartolini, Phys. Rev. 159, 1022 (1967).

[16]G. Chodil, R. C. Jopson, H. Mark, C. D. Swift, R. G. Thomas, and M. K. Yates, Nucl. Phys. A93, 648 (1967).

[17]P. P. Dmitriev, I. O. Konstantinov, and N. N. Krasnov, At. Energ. (USSR) 22, 310 (1967) [transl.: Sov. J. At. Energy 22, 386 (1967).

[18]M. Hille, P. Hille, M. Uhl, and W. Weisz, Nucl. Phys. A198, 625 (1972).

[19]C. H. Johnson, A. Galonsky, and J. P. Ulrich, Phys. Rev. 109, 1243 (1958).

[20]B. W. Shore, N. S. Wall, and J. W. Irvine, Jr., Phys. Rev. 123, 276 (1961).

[21]J. Wiley, J. C. Pacer, C. R. Lux, and N. T. Porile, Nucl. Phys. A212, 1 (1973).

[22]G. B. Saha, N. T. Porile, and L. Yaffe, Phys. Rev. 144, 962 (1966); D. R. Sachdev, N. T. Porile, and L. Yaffe, Can. J. Chem. 45, 1149 (1967).

[23]J. J. Hogan, Phys. Rev. C 6, 810 (1972).

[24]See, for example, Refs. 22 and 23; V. P. Narang and L. Yaffe, Can. J. Chem. 46, 3171 (1968); J. J. Hogan, J. Inorg. Nucl. Chem. 35, 705, 1429 (1973) and additional references quoted therein.

[25]N. Metropolis, R. Bivins, M. Storm, A. Turkevich, J. M. Miller, and G. Friedlander, Phys. Rev. 110, 185, 204 (1958).

[26]K. Chen, Z. Fraenkel, G. Friedlander, J. R. Grover, J. M. Miller, and Y. Shimamoto, Phys. Rev. 166, 949 (1968).

[27]K. Chen, G. Friedlander, and J. M. Miller, Phys. Rev. 176, 1208 (1968).
[28]K. Chen, G. Friedlander, G. D. Harp, and J. M. Miller, Phys. Rev. C 4, 2234 (1971).
[29]J. R. Grover and J. Gilat, Phys. Rev. 157, 802 (1967).
[30]D. G. Sarantites and B. D. Pate, Nucl. Phys. A93, 545 (1967); D. G. Sarantites, *ibid.* A93, 567 (1967).
[31]F. H. Ruddy, B. D. Pate, and E. W. Vogt, Nucl. Phys. A127, 323 (1969).
[32]M. Uhl, Acta Phys. Austriaca 31, 245 (1970).
[33]J. J. Griffin, Phys. Rev. Lett. 17, 478 (1966); M. Blann, *ibid.* 21, 1357 (1968); W. W. Bowman and M. Blann, Nucl. Phys. A131, 513 (1969); M. Blann and F. M. Lanzafame, *ibid.* A142, 559 (1970).
[34]C. K. Cline and M. Blann, Nucl. Phys. A172, 225 (1971); M. Blann and A. Mignerey, *ibid.* A186, 245 (1972).
[35]F. Ajzenberg-Selove, Nucl. Phys. A152, 1 (1970).
[36]J. B. Cumming, Nucl. Phys. 49, 417 (1963).
[37]L. C. Northcliffe and R. F. Schilling, Nucl. Data A7, 233 (1970).
[38]C. F. Williamson, J. P. Boujot, and J. Picard, Centre d'Études Nucléaires de Saclay Report No. CEA-R3042, 1966 (unpublished).
[39]Energy straggling was estimated by the Bohr treatment [N. Bohr, Phil. Mag. 30, 581 (1915)] which, although energy-independent, is a good approximation for energy losses from 1 to 15%. For the absorbers and energy range of interest in this work, it is also in reasonable agreement with the more accurate but more tedious Bethe range straggling procedure [M. S. Livingston and H. A. Bethe, Rev. Mod. Phys. 9, 264 (1937)]. See, for example, H. Bichsel and E. A. Uehling, Phys. Rev. 119, 1670 (1960); R. M. Sternheimer, *ibid.* 117, 485 (1960); H. Nann and W. Schäfer, Nucl. Instrum. Methods 100, 217 (1972).
[40]S. C. Pancholi and K. Way, Nucl. Data B2 (No. 6), 1 (1968).
[41]I. Borchert, Z. Phys. 223, 473 (1969).
[42]F. E. Bertrand and D. J. Horen, Nucl. Data B7, 1 (1972).
[43]R. S. Hager and E. C. Seltzer, Nucl. Data A4, 1 (1968).
[44]R. Collé and R. Kishore, to be published.
[45]R. Gunnink, H. B. Levy, and J. B. Niday, University of California Radiation Laboratory Report No. UCID-15140 (unpublished); modified by B. R. Erdal (unpublished).
[46]J. B. Cumming, National Academy of Sciences-National Research Council Nuclear Science Series Report No. NAS-NS-3107, 1962 (unpublished).
[47]R. L. Aamodt, V. Peterson, and R. Phillips, Phys. Rev. 88, 739 (1952).
[48]F. K. McGowan, W. T. Milner, and H. J. Kim, Oak Ridge National Laboratory Report No. ORNL-CPX-2, 1964 (unpublished).
[49]D. A. Newton, S. Sarkar, L. Yaffe, and R. B. Moore, J. Inorg. Nucl. Chem. 35, 361 (1973).
[50]L. A. Konig, J. H. E. Mattauch, and A. H. Wapstra, Nucl. Phys. 31, 18 (1962).
[51]G. S. Mani, M. A. Melkanoff, and I. Iori, Centre d'Études Nucléaires de Saclay Report No. CEA-2379, 1963 (unpublished).
[52]The goodness-of-fit parameter ($\hat{\sigma}$) is given by the square root of the weighted sum of the residuals divided by the degrees of freedom (ν), i.e., $\hat{\sigma}=[(\sum_i(\bar{x}-x_i)^2/\sigma_i^2)/\nu]^{1/2}$; cf., W. C. Hamilton, *Statistics in Physical Science* (Ronald Press, New York, 1964), p. 130.
[53]F. Strassmann and E. Walling, Ber. Deut. Chem. Ges. 71B, 1 (1938).
[54]O. Huber, H. Medicus, P. Preiswerk, and R. Steffen, Helv. Phys. Acta 20, 495 (1947).
[55]H. Wäffler and O. Hirzel, Helv. Phys. Acta 21, 200 (1948).
[56]C. V. Strain, Phys. Rev. 54, 1021 (1938).
[57]W. Bothe and W. Gentner, Z. Phys. 112, 45 (1939).
[58]L. A. Delsasso, L. N. Ridenour, R. Sherr, and M. G. White, Phys. Rev. 55, 113 (1939).
[59]R. A. Ricci, R. K. Girgis, and R. van Lieshout, Nuovo Cimento 11, 156 (1959).
[60]I. L. Preiss and R. W. Fink, Nucl. Phys. 15, 326 (1960).
[61]L. A. Rayburn, Phys. Rev. 122, 168 (1961).
[62]S. S. Vasilev, No Haieng Chang, and L. Ya. Shavtvalov, Zh. Eksp. Teor. Fiz. 40, 475 (1961) [transl.: Sov. Phys. JETP 13, 331 (1961)].
[63]J. B. Cumming and N. T. Porile, Phys. Rev. 122, 1267 (1961).
[64]V. A. Paulsen and H. Liskien, Nukleonik 7, 117 (1965).
[65]J. Goss, F. Riffle, D. Parsignault, and J. C. Harris, Bull. Am. Phys. Soc. 12, 535 (1967).
[66]A. C. Helmholz, Phys. Rev. 60, 415 (1941).
[67]G. E. Valley and R. L. McCreary, Phys. Rev. 56, 863 (1939).
[68]N. L. Lark, P. F. A. Goudsmit, J. F. W. Jansen, J. E. J. Oberski, and A. H. Wapstra, Nucl. Phys. 35, 582 (1962).
[69]C. M. Lederer, J. M. Hollander, and I. Perlman, *Table of Isotopes* (Wiley, N. Y., 1967), 6th ed.; W. Seelmann-Eggebert, G. Pfennig, and H. Münzel, *Nuclidkarte* (Bundesminister für Wissenschaftliche Forschung, Bonn, 1968), 3rd ed.